A Model for Flow Regime Transitions in Cocurrent Down-flow Trickle-bed Reactors

A study of the nature of interstitial flows within trickle-bed reactors is presented. Based on physical concepts, a theory is developed to predict the transition boundaries for various flow regimes for nonfoaming liquids. The effects of factors such as bed porosity, size of monodispersed spherical catalyst particles, interfacial tension, viscosity, density, and the gas and liquid flow rates, on flow transitions are considered. Experimental data in the literature are used to confirm the theory and the agreement is good.

K. M. NG

Chemical Engineering Department
University of Massachusetts
Amherst, MA 01003

SCOPE

In the design and scale-up of cocurrent down-flow trickle-bed reactors, it is imperative to predict which flow regime to expect for a given reactor system and a specified set of operating conditions, since the flow pattern may significantly affect the reactor performance. The present approach relies heavily on empirical flow maps, a typical example of which is a plot of gas flow rate vs. liquid flow rate, with the observed flow regime indicated on the plot for all flow rate combinations. Although this direct approach provides useful information, there are two major drawbacks. First, most flow maps are derived from pilot-scale reactor data and are valid only within a narrow range of operating conditions, usually moderate temperature and pressure, under which the data are obtained. Second, these flow maps do not demonstrate the interplay of various factors such as wettability, interfacial tension, viscosity, bed porosity, and others, on transitions between flow regimes.

To resolve this difficulty it is the objective of this paper to put these flow maps on a theoretical basis by providing analytical predictions of flow regime transitions. Six flow regimes are considered: partial wetting trickle flow, complete wetting trickle flow, pulsing flow, spray flow, and bubble and dispersed bubble flows.

CONCLUSIONS AND SIGNIFICANCE

A model is developed to predict the flow regime map for a given reactor system and a specific set of operating conditions. It has two major components: a porous medium model for granular beds and physical mechanisms for flow transitions. To generate such a flow map, physical parameters such as packing particle size, bed porosity, pressure, temperature, and others are the only required inputs, a list of which is shown in both Tables 1 and 2. The five transition curves designated by different letters of the alphabet, and the equations for calculating them are summarized below.

A. Partial wetting to complete wetting, Eqs. 8 and 9
B. Trickling to pulsing, Eqs. 11–14
C. Trickling to spray, Eqs. 15 and 16
D. Trickling/pulsing to bubble, Eqs. 17–20
E. Bubble to dispersed bubble, Eq. 23

The geometrical characteristics of the bed such as average pore size needed in the equations for flow transitions are given by Eqs. 3–7.

The model is tested against literature data, Figure 4. The agreement is good. The sensitivity of the model to changes in physical parameters such as porosity (Figure 5), interfacial tension (Figure 6), and packing particle size (Figure 7) is also found to be in agreement with experimental data.

Based on this model, the flow map for a high-pressure air-water system is calculated (Figure 8). It shows that the flow map for a high-pressure system deviates significantly from that of a low-pressure, pilot-scale unit, from which flow maps are usually generated.

Thus, this more rigorous hydrodynamic model of the bed allows a priori prediction of a flow regime map. In addition, it provides a framework for correlating flow regime data, furnishes a basis to move out into regions where experimental data are not available, and elucidates the effects of various physical factors on flow transitions.

INTRODUCTION

Various flow regimes may exist in cocurrent gas-liquid downflow trickle-bed reactors: trickling, pulsing, spray, and bubble flows. Due to the vast difference in the hydrodynamic characteristics of these regimes, the respective heat and mass transfer rates, holdup, and pressure drop also differ in a significant way. For this reason, in the design or scale-up of trickle-bed reactors it is imperative to predict which flow regime to expect for a given reactor system and a specified set of operating conditions.

The present approach relies heavily on empirical flow regime maps that have been developed in the last two decades (Weekman and Myers, 1964; Beimesch and Kessler, 1971; Sato et al., 1973; Charpentier and Favier, 1975; Talmor, 1977; Fukushima and Kusaka, 1977). However, because of the large number of variables such as bed porosity, size and shape of catalysts, viscosity, density, interfacial tension, reactor dimensions, flow rates, etc., that seem to have an important effect on the bed operation, most existing flow maps are valid only within the range of conditions under which the data were obtained.

To resolve this difficulty, it is desirable to put the flow maps on a theoretical basis. In this paper, a hydrodynamic model of the bed is formulated to provide a framework for correlating data and to delineate the interplay of the various factors mentioned above on flow transitions.

Before proceeding further, it is of interest to point out that the flow phenomena in trickle beds are not unlike those in pipes, in that similar flow regimes are present in both cases. The major difference is that the trickle-bed problem is further complicated by the random pore structure.

In following the progress of research in gas-liquid two-phase flow in pipes, we find that the research has gone through a period of empiricism—for instance, constructing flow regime maps and correlating pressure-drop data (Baker, 1954; Lockhart and Martinelli, 1949). It is not surprising that many of those ideas have been employed in correlating packed-bed data. In the last decade, however, more fundamental advances have been made in pipe flows. In particular, the papers by Taitel and Dukler (1976) and Taitel et al. (1980) on flow regime transitions in pipes have provided the inspiration for this work.

FLOW DESCRIPTION

The four basic flow regimes in trickle-bed reactors are briefly described below. Only those features of relevance to this work are discussed and discussion is based on the results and observations of the previously mentioned investigators. For readers who are unfamiliar with this area, it may be of help to examine a typical flow regime map at the same time (Figure 4).

Trickling Flow Regime

In trickling flow the liquid flows down the column on the surface of the packings while the gas phase travels in the remaining void space. The flow regime can be divided into two regions. At low gas and liquid flow rates, the liquid flow is laminar and a fraction of the packing remains unwetted. If the liquid rate is raised, the partial wetting regime changes to complete wetting trickling regime in which the packing is totally covered by a liquid film. Figure 1a shows such a situation at a certain location inside the bed. The circles represent the catalyst particles, which of course touch some other contiguous particles.

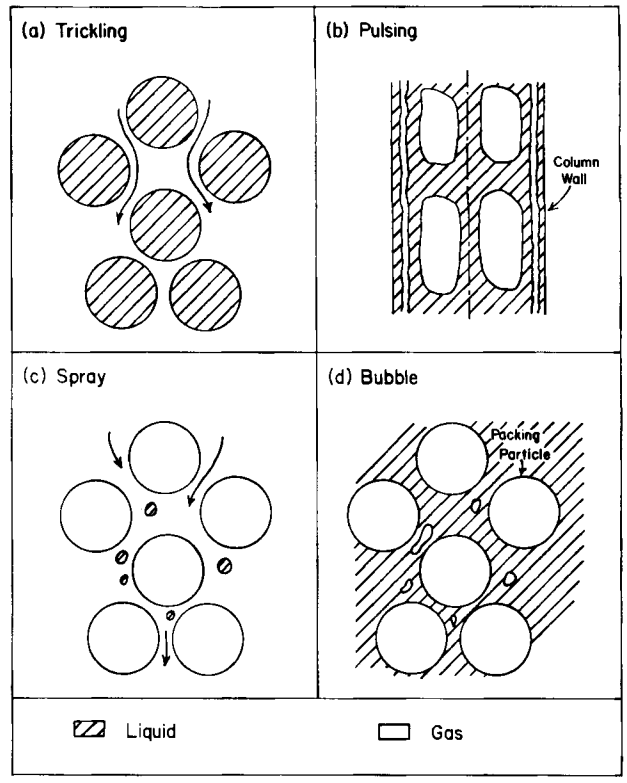

Figure 1. Flow patterns in trickle beds.

Pulsing Flow Regime

The pulsing behavior refers to gas and liquid slugs traversing the column alternately at high gas and liquid flow rates. It begins when the flow channels between packings are plugged by a slug of liquid, followed by blowing off of the slug by the gas flow. Pulses always begin at the bottom of the bed, as the gas velocity is higher there due to lower pressure. As the gas flow rate is increased, the incipient point of pulsing moves to the upper part of the column. Figure 1b represents what one may see in a pilot-scale column; the packing particles are not shown. It should be noted that the gas pulse is not completely devoid of liquid. A thin film of liquid always exists on the surface of the packings within the gas pulse. Similarly, the liquid pulse also contains some small gas bubbles, particularly at the front end of the liquid pulse.

Spray Flow Regime

Transition to the spray flow regime occurs when the gas flow rate is high while the liquid flow rate is kept at a low value. The liquid phase travels down the column in the form of droplets entrained by the continuous gas phase (Figure 1c).

Bubble/Dispersed Bubble Flow Regimes

The bubble flow regime appears at high liquid flow rates and low gas flow rates. The entire bed is filled with the liquid and the gas phase is in the form of slightly elongated bubbles (Figure 1d). If the gas flow rate is increased, the bubbles become highly irregular in shape. This is referred to as the dispersed bubble regime.

THE POROUS MEDIUM MODEL

A suitable mathematical model for the bed is needed to account for the interaction between the fluids and the catalysts. In this work, we will limit our attention to a random packing of equal-size, spherical particles.

Consider a packed column of porosity, ε, consisting of spherical catalyst of diameter, d_g. If a horizontal cut is made across the bed, the size distribution of the circles of diameter x on the sectional plane, $f(x)$, is given by (Appendix)

$$f(x) = \frac{x}{d_g\sqrt{d_g^2 - x^2}} \tag{1}$$

If N_c is the number of circles per unit area, we can calculate the fractional area of the column occupied by the spherical particles as follows

$$N_c \int_o^{d_g} \frac{\pi}{4} x^2 f(x) dx = (1 - \varepsilon) \tag{2}$$

Hence, we obtain, after integration of Eq. 2

$$N_c = \frac{6(1 - \varepsilon)}{\pi d_g^2} \tag{3}$$

Then, the length of grain boundary per unit sectional area, S, is given by

$$S = \int_o^{d_g} \pi x N_c f(x) dx = \frac{\pi^2}{4} d_g N_c \tag{4}$$

We will also need the average flow channel diameter, $\langle d_c \rangle$, and average pore diameter, $\langle d_p \rangle$, of the packed bed. For packed columns of equal spheres, the number of flow channels per unit area is approximately the same as the number of circles on a sectional plane (Payatakes et al., 1973). Hence, the former can be obtained by

$$\frac{\pi\langle d_c\rangle^2}{4} N_c = \varepsilon \quad \text{or} \quad \langle d_c \rangle = \sqrt{\frac{4\varepsilon}{\pi N_c}} \tag{5}$$

It should be noted that $\langle d_c \rangle$ represents the average size, expressed in terms of an equivalent diameter, of a flow channel that consists of relatively large pore chambers and small pore throats. Obviously, $\langle d_c \rangle$ is larger than the constrictions and is less than $\langle d_p \rangle$, which can be obtained by

$$\frac{\langle d_p\rangle^3}{d_g^3} = \frac{\varepsilon}{(1 - \varepsilon)} \quad \text{or} \quad \langle d_p \rangle = \left(\frac{\varepsilon}{1 - \varepsilon}\right)^{1/3} d_g \tag{6}$$

Another interesting feature is the minimum throat diameter of the bed, $d_{t,\min}$. It is known that the smallest constriction within such a packed bed is the one formed by three spheres in contact, and its area can be calculated by subtracting the area of the three circular sectors from that of the equilateral triangle formed by joining the centers of the three touching spheres. Thus, the equivalent diameter of the minimum throat is given by

$$d_{t,\min} = \sqrt{\frac{2}{\pi} \sin\frac{\pi}{3} - \frac{1}{2}}\, d_g \tag{7}$$

All these geometrical features, as will be seen below, are of significance to flow transitions.

FLOW REGIME BOUNDARIES

The following analysis is intended for nonfoaming systems. The physics of foaming systems is more complex and will not be considered in this work.

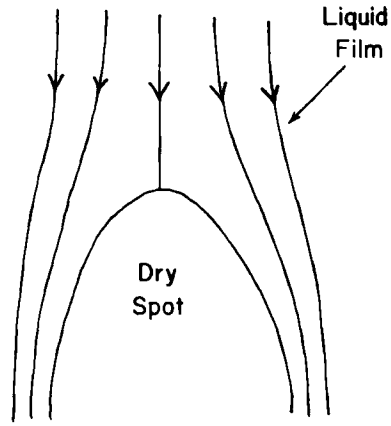

Figure 2. Dry patch model (after Hartley and Murgatroyd, 1964).

Transition from Partial Wetting to Complete Wetting in the Trickle Flow Regime

In the partial wetting trickling regime, the laminar liquid films flow on the solid surfaces and a fraction of the packing is unwetted. In the case of porous catalysts, the meaning of dewetting has to be taken as the absence of a continuous liquid film covering the entire solid surface, because a small amount of liquid is always present due to the capillary effect.

Now, consider the following situation. A laminar thin film of liquid flows down a vertical wall. The liquid rate is not high enough and a dry spot is formed (Figure 2). At the stagnation point, the liquid changes direction and its kinetic energy is converted into stagnation force that tends to push the contact line downward. The contact line is still pinned on the wall because of the surface tension force. Based on this dry patch model, Hartley and Murgatroyd (1964) suggested that the minimum flow rate per unit length, m, above which the stagnation force is always greater than the surface tension effect is proportional to the physical properties of the system in the following manner.

$$m \propto \left(\frac{\mu_l \rho_l}{g}\right)^{1/5} \sigma^{3/5} \tag{8}$$

The experimental data of Norman and McIntyre (1960) indicate that the proportionality constant is of the order of 0.1. Here, μ and ρ are viscosity and density respectively, g is the acceleration due to gravity, and σ is the interfacial tension.

Applying this concept to the packed bed, the minimum superficial mass flow rate of liquid, L, to attain complete wetting can be estimated by multiplying the flow rate per unit length with the total length of grain boundary per unit sectional area. Thus

$$L = m S \tag{9}$$

Equation 9 gives the transition curve from partial wetting to complete wetting in a flow regime map. It should be noted that, strictly speaking, Eq. 8 only holds at the equator of a sphere where the tangents are vertical. Since S represents the circumferential length of circles formed by cutting each sphere at any position along the sphere axis, Eq. 9 is not exact, although it is expected to yield a satisfactory estimate. In fact, the amount of liquid required to wet the walls of the packed column is also not considered in this analysis. Further work taking into account these secondary but more complete aspects is under way.

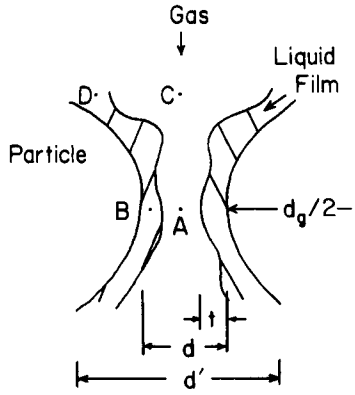

Figure 3. Instability of liquid films momentarily before the formation of a liquid pulse.

Transition from Trickling to Pulsing Flow

For transition from trickling to pulsing flow, the liquid slug is initiated just above the constrictions of the porous medium. This is because the gas velocity is the highest there. Figure 3 depicts that at a typical constriction in the packed bed the gas flow induces the formation of a bridge between the liquid films on two separate particles, whereas the surface tension force tends to keep them apart. Applying Bernoulli's concept, we get

$$\frac{1}{2}\rho_g u_g^2 + p_A = \frac{1}{2}\rho_g u_g'^2 + p_C \tag{10}$$

where u_g, u_g', are interstitial velocities at points A and C, respectively, and p is pressure. Equation 10 is not valid for turbulent flows although, as demonstrated in a similar analysis by Taitel and Dukler (1976), it is expected to yield a reasonable estimate over a short distance such as d_g in this case.

At the time just before the films collapse and form a pulse, the downward liquid flow is momentarily stalled and then proceeds to move inward to close the constriction. At that very moment, the film can be considered to be stationary and the pressures at locations B and D are simply related by the hydrostatic head, that is, $p_D = p_B - \rho_l g d_g/2$. It can also be seen that p_C is of the magnitude of p_D, since there is no curvature there, and that $p_B - p_A = 4\sigma/d_g$ by the Young-Laplace equation. Substituting these equations and the continuity equation $u_g d^2 = u_g' d'^2$ into Eq. 10, we get

$$\frac{1}{2}\rho_g u_g^2\left[1 - \left(\frac{d}{d'}\right)^4\right] = \frac{4\sigma}{d_g} - \rho_l g\frac{d_g}{2} \tag{11}$$

Here d and d' are the diameters of the constriction and wider pore chamber respectively. Since d is slightly less than $\langle d_c\rangle$ and d' is close to $\langle d_p\rangle$, we conclude that (d/d') is on the order of 0.3 to 0.5 for a sphere pack of equal sizes (Payatakes et al., 1973). Hence, $(d/d')^4 << 1$ and can be neglected.

Once u_g is known, the superficial mass flow rate of gas, G, for pulsing flow to occur is obtained by multiplying the area per unit column area open for gas flow $\varepsilon(1 - \alpha)$ by the velocity u_g and gas density.

$$G = \varepsilon u_g(1 - \alpha)\rho_g \tag{12}$$

where α is the fraction of flow channels occupied by the liquid films and α is related to the average liquid saturation in the bed, β, by (Appendix)

$$\alpha = 4[\sqrt{1 - \beta} - (1 - \beta)] \tag{13}$$

At this stage, theoretical prediction of β is impossible and a correlation by Wijffels et al. (1974), as shown below, can be used.

$$\beta = \left[\left(\frac{200}{Re_l} + 1.75\right)\frac{v_l^2}{g d_g}\frac{1 - \varepsilon}{\varepsilon^3}\right]^{1/4} \tag{14}$$

Here, v_l is the superficial velocity of the liquid, Re_l is the Reynolds number $(\rho_l v_l d_g/\mu_l)$.

Equations 11 through 14 provide the transition curve from trickling to pulsing flow. To be more exact, for each value of the superficial mass flow rate of liquid, L, v_l is given by L/ρ_l and can be calculated. Then, β is calculated using Eq. 14. Substituting u_g from Eq. 11 and α from Eq. 13 into Eq. 12 yields the corresponding value of the superficial mass rate of gas, G.

It should be mentioned that this analysis is not valid for large catalyst particles on the order of 1 cm dia. In that case, the films would form waves which do not correspond to the curvature of the catalyst particle. Consequently, the equation $p_B - p_A = 4\sigma/d_g$ no longer holds and mechanisms for flow transition in pipes are more appropriate (Barnea et al., 1982).

Transition from Trickling to Spray Flow

The transition from trickling to spray flow occurs when the gas flow rate is increased. The liquid film is shattered and liquid droplets are entrained in the continuous gas phase down the column. The size of the droplet depends on the surface tension that holds the droplet intact and the turbulent flow that tends to shatter it. We propose that the turbulent impact force has to be able to keep the droplet size less than $d_{t,\min}$ at the point of transition. Otherwise the droplets would be stopped at the constrictions and form liquid films. The surface tension pressure is proportional to $\sigma/d_{t,\min}$, using the Young-Laplace equation. The impact pressure is proportional to $\rho_g u_g^2$. This leads to the following proportionality relationship.

$$u_g \propto \sqrt{\frac{\sigma}{\rho_g d_{t,\min}}} \tag{15}$$

Based on experimental data, Hinze (1955) determined the proportionality constant to be about 5. Then, the superficial mass flow rate of gas can be calculated as the product of the area per unit column area open for gas flow, $\pi d_{t,\min}^2 N_c/4$, and the velocity and gas density.

$$G = \frac{\pi}{4} d_{t,\min}^2 N_c u_g \rho_g \tag{16}$$

With N_c calculated from Eq. 3, $d_{t,\min}$ from Eq. 7 and u_g from Eq. 15, Eq. 16 gives the transition curve from trickling to spray flow in a flow regime map.

Transition from Trickling/Pulsing to Bubble Flow

We suggest that this transition takes place when the turbulent fluctuations of the liquid are able to keep the bubble size below the average pore size. Otherwise, the bubble is indeed either a gas pulse in the pulsing regime or a continuous phase in the trickling regime.

The size of a drop in turbulent flow is of order of magnitude of $(\sigma/\rho_l)^{3/5} e^{-2/5}$ (Levich, 1962). Here, e is the rate of energy dissipation per unit mass of liquid. Hinze (1955) and Sevik and Park (1973) determined the proportionality constant to be 1.15. Thus, we have

$$\langle d_p\rangle = 1.15\left(\frac{\sigma}{\rho_l}\right)^{3/5} e^{-2/5} \tag{17}$$

for relatively small gas holdup. e can be calculated by (Taitel et al., 1980)

$$e = \frac{v_l}{\rho_l}\left|\frac{dp}{dz}\right| \tag{18}$$

The pressure drop $|dp/dz|$ can be calculated by the Ergun equation (Bird et al., 1960):

$$\left|\frac{dp}{dz}\right| = \frac{150\mu_l v_l}{d_g^2}\frac{(1-\varepsilon)^2}{\varepsilon^3} + 1.75\frac{\rho_l v_l^2(1-\varepsilon)}{d_g\varepsilon^3} \tag{19}$$

Combining Eqs. 18 and 19, and substituting into Eq. 17 yields one equation with v_l as the only unknown, the value of which can be readily determined. The minimum superficial liquid mass flow rate is simply the product of superficial velocity and density

$$L = v_l\rho_l \tag{20}$$

Equation 20 gives the transition curve from trickling/pulsing to bubble flow in a flow regime map.

Transition from Bubble to Dispersed Bubble Flow

Another feature of the bubble flow regime needs to be mentioned. Consider that the liquid rate is high enough so that we are in the bubble regime. The bubbles are slightly elongated but are more or less spherical. If the gas flow rate is gradually increased, the gas holdup will also increase up to the point at which the volume fraction of the bubbles is the same as that of the liquid. This means that $\beta = 0.5$. To accommodate this quantity of gas holdup, the bubbles become very irregular in shape. This is known as the dispersed bubble regime. The transition curve can be obtained as follows.

The interstitial velocities of gas and liquid are given by

$$u_g = \frac{v_g}{\varepsilon(1-\beta)} \tag{21}$$

and

$$u_l = \frac{v_l}{\varepsilon\beta} \tag{22}$$

In dispersed bubble flow, u_g is approximately equal to u_l, as the gas and liquid phases are very well mixed. Equating Eqs. 21 and 22, and using the relationships $G = v_g\rho_g$ and $L = v_l\rho_l$, leads to

$$G = \frac{1-\beta}{\beta}\frac{\rho_g}{\rho_l}L \tag{23}$$

As pointed out above, β is approximately equal to 0.5 at the transition curve. (This number corresponds to the void fraction of a random packing of equal-size spheres, which is about 0.4.) Equation 23 gives the transition curve from bubble to dispersed bubble flow in a flow regime map.

COMPARISON OF MODEL PREDICTIONS WITH LITERATURE DATA

Most flow regime maps in the literature are based on data obtained from pilot scale columns of 0.5 ft. (15 cm) or less in diameter and of moderate operating conditions. In general, the data from different investigators seldom completely agree with one another. This is due to the fact that they may use different criteria to determine the point at which transition takes place. For instance, visual observations (Sato et al., 1973) and wall pressure fluctuations (Chou et al., 1977) have been employed. For this reason, literature data are subject to the interpretation

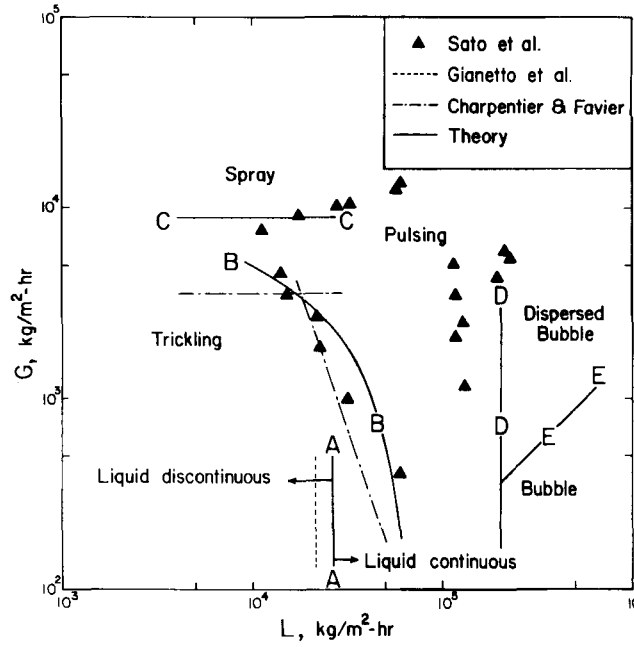

Figure 4. Comparision of theory and experiment in a flow map for a typical pilot-scale trickle-bed reactor.

of the experimentalists and should be viewed as indicative rather than definitive.

The properties of an air-water system in a typical pilot-scale trickle-bed reactor are listed in Table 1. Experimental data for this system from various sources and the predicted transition curves are shown in Figure 4.

Curve A is the predicted transition boundary between partial wetting and complete wetting and is obtained from Eq. 9. Gianetto et al. (1978) suggested a liquid flow rate greater than 2.2×10^4 kg/m^{2}h to attain complete wetting, which is reasonably close to our prediction.

The trickling-pulsing transition boundary (curve B and Eq. 12 lies somewhat above the data of Sato et al. (1973) and Charpentier and Favier (1975). The trickling-spray transition boundary (curve C) is obtained from Eq. 16 and is also close to their data.

Curve D (Eq. 20) indicates the liquid flow rate above which bubble flow occurs, which is slightly higher than Sato's data. Curve E (Eq. 23) separates the bubble regime and the dispersed bubble regime. Reliable experimental data for this boundary have not been found. However, it coincides with the data in a flow map in Froment and Bischoff (1979) even though the source of the original data is not clear.

TABLE 1. PROPERTIES AND OPERATING CONDITIONS OF A TYPICAL PILOT-SCALE TRICKLE-BED SYSTEM

d_g	0.5 cm
ε	0.4
p	1.5 atm
T	25°C
ρ_l	1×10^3 kg/m^3
μ_l	1×10^{-3} N · s/m^2
ρ_g	1.8 kg/m^3
σ	7.2×10^{-2} N/m

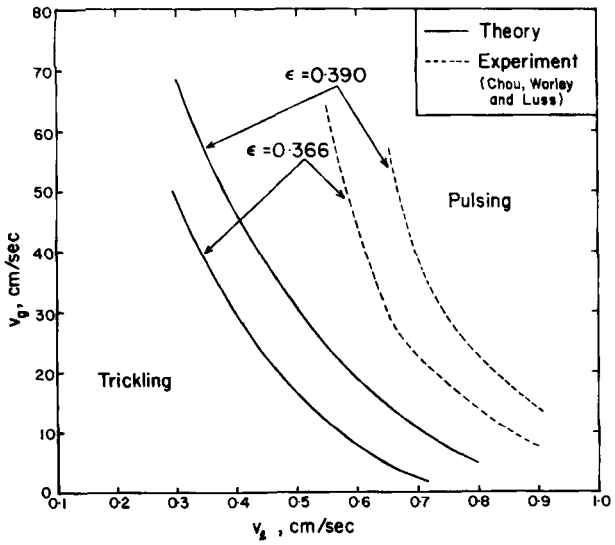

Figure 5. Comparison of theory and experiment on the effect of bed porosity on the trickling-pulsing transition boundary.

Effects of Porosity, Surface Tension, and Particle Size

Figure 5 shows the effect of porosity on the trickling-pulsing transition. Although the predicted curves do not coincide with the experimental data of Chou et al. (1977) for 0.29 cm particles, the relative shift resulting from changed porosity is the same for both the theory and the experiment. These data correspond to the lower half of the trickling-pulsing boundary shown in Figure 4. Note that the change in shape of the theoretical curves, from convex in Figure 4 to concave in Figure 5, is because Figure 4 is a log-log plot and thus does not represent any physical significance. Also, the predicted curve for porosity 0.39 lies below the experimental data of Chou et al., in contrast to the previous case, where the predicted curve is above the data of Sato et al. and Charpentier and Favier.

The effect of surface tension on the trickling-pulsing boundary is shown in Figure 6. Again, the data are due to Chou et

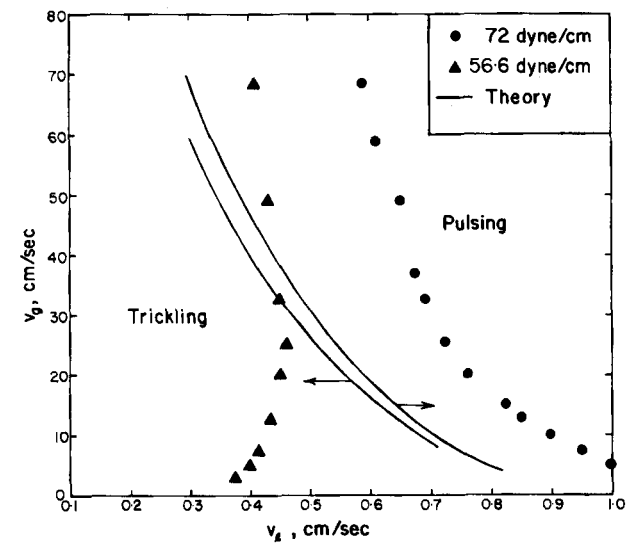

Figure 6. Comparison of theory and experiment on the effect of surface tension on the trickling-pulsing transition boundary.

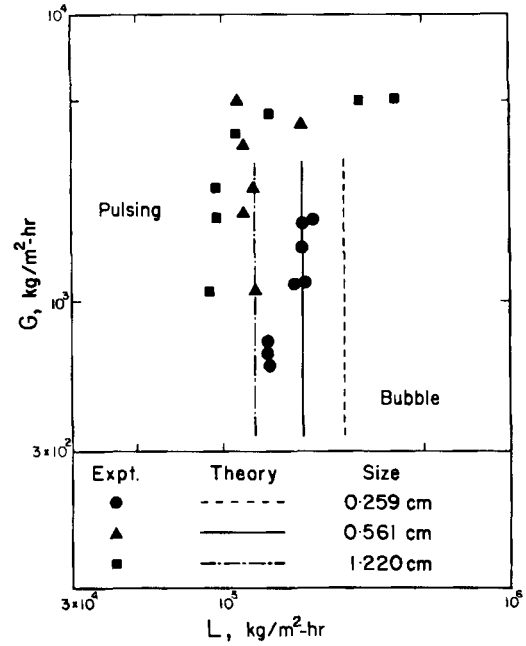

Figure 7. Comparison of theory and experiment on the effect of particle size on the pulsing-bubble flow transition boundary.

al. As can be seen, the theory predicts a very small shift whereas the data indicate a much larger one. However, the peculiar shape of the experimental curve at 5.66×10^{-2} N/m leads us to believe, as was suggested by the original authors, that factors other than surface tension, such as weak foaming, are the cause for the large shift in the experimental data.

In Figure 7, the data of Sato et al. for the trickling/bubble flow boundary are plotted for three different particle sizes. Although all three predicted curves lie to the right of the data, the relative shifts in the theoretical and experimental results are in good agreement.

DISCUSSION

It has been repeatedly stressed by different researchers that flow regime transitions are not well understood and the effects of various parameters on flow boundaries are uncertain (Chou et al. 1977; Sicardi et al., 1979). To meet the need, this work is an attempt to provide a physical picture of the flow behavior.

After gaining confidence by confirming the theory with literature data, it is of interest to move into regions where experimental data do not exist. Motivated by the fact that commercial hydrodesulfurization trickle-bed reactors may be operated at up to 70 atm (7.1 MPa) and 400°C, a flow map for an air-water system at higher temperature and pressure is presented in Figure 8. The properties of the system are given in Table 2.

Several features are noteworthy. As expected, curves B, C, and E are much higher than the corresponding curves at a lower temperature and pressure. This is mainly due to the significant increase in air density. However, the relative shift in E and E' is much bigger than the shift in B and B', and C and C'. This is not surprising since an examination of the flow transition equations reveals that curve E is proportional to ρ_g while curves B and C are both proportional to the square root of ρ_g. The slight decrease in surface tension, from 7.2×10^{-2} to 6.44×10^{-2} N/m resulting from the increase in temperature has left curves A and D virtually unchanged.

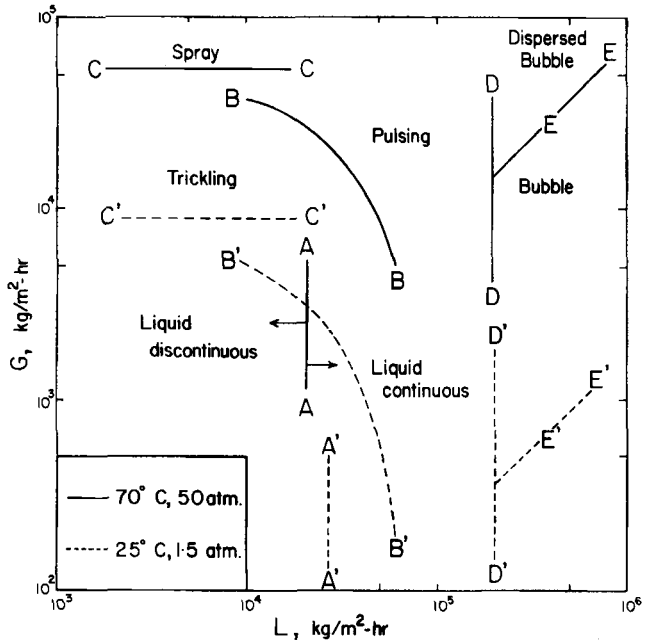

Figure 8. The predicted effect of higher temperature and pressure on a flow map.

TABLE 2. PROPERTIES AND OPERATING CONDITIONS OF A HYPOTHETICAL TRICKLE-BED SYSTEM

d_g	0.5 cm
ε	0.4
p	50 atm
T	70°C
ρ_l	1×10^3 kg/m^3
μ_l	4×10^{-4} N · s/m^{-2}
ρ_g	73 kg/m^3
σ	6.44×10^{-2} N/m

Figure 8 also clearly demonstrates the caution one should exercise in using flow maps in the literature. Consider the area between curves B and B'. What appears to be a pulsing regime may indeed be a trickling regime in a high-pressure system. Of course this is in complete agreement with the usual observation that incipient pulsing always begins at the bottom of the column.

The fact that two different flow regimes can coexist leads to an important caveat in applying this theory to large reactors. The present model has assumed uniform pressure and temperature but, indeed, the pressure may decrease significantly in a large reactor. However, since this model is valid at each point inside the reactor, one possible approach is to determine the pressure drop and the flow regime step by step down the bed. Results of the work along this line have been reported elsewhere (Dimenstein et al., 1984).

ACKNOWLEDGMENT

This work was performed under National Science Foundation Grant CPE-8209920. The author also thanks J. M. Douglas for valuable and stimulating discussions throughout the course of this work.

NOTATION

A,B,C,D = locations in Figure 3
d = throat diameter in Figure 3
d' = diameter of the pore chamber in Figure 3
$\langle d_c \rangle$ = average diameter of flow channels
d_g = particle diameter
$\langle d_p \rangle$ = average diameter of pore chambers
$d_{t,\min}$ = minimum throat diameter in the column
e = energy dissipation per unit mass of liquid
$F(x)$ = fraction of circles of diameter less than x on a sectional plane
$f(x)$ = frequency distribution of circles on a sectional plane
G = superficial mass flow rate of gas
g = acceleration due to gravity
L = superficial mass flow rate of liquid
m = minimum flow rate per unit length for complete wetting
N_c = number of circles irrespective of size per unit sectional area
p = pressure
Re = Reynolds number
S = length of grain boundary per unit sectional area
t = liquid film thickness in the throat in Figure 3
$\langle t \rangle$ = liquid film thickness in an average pore chamber
u = interstitial velocity
v = superficial velocity
X,Y = locations in Figure 9
x = diameter of circle on a sectional plane
z = axial coordinate along the bed

Greek Letters

α = fraction of the throat area occupied by liquid
β = liquid saturation
ε = porosity
μ = viscosity
ρ = density
σ = surface tension

Subscripts

g = gas phase
l = liquid phase

APPENDIX: DERIVATION OF EQS. 1 AND 13

Consider that a horizontal cut is made through an array of randomly packed spheres of a uniform size. If the packing is totally random, the fraction of circles of diameter less than x, $F(x)$, can be obtained using a single sphere as follows (Figure 9).

$$F(x) = \frac{XO - YO}{XO} = \frac{d_g - \sqrt{d_g^2 - x^2}}{d_g} \tag{A1}$$

Equation A1 is based on the facts that any horizontal cut across the line XY would give a circle of diameter x or less and that the line OX represents all the possible locations of a cut. The lower half of the sphere is symmetric to the upper half and does not need to be considered in the determination of $F(x)$.

The frequency distribution of circles, $f(x)$, is given by

$$f(x) = \frac{dF(x)}{dx} = \frac{x}{d_g\sqrt{d_g^2 - x^2}} \tag{A2}$$

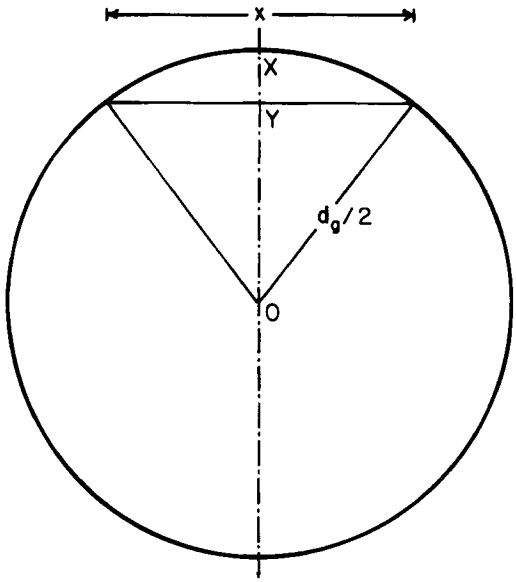

Figure 9. Derivation of Eq. 1.

To obtain Eq. 13, let t be the film thickness in the narrower pore mouth. Referring back to Figure 3, we have

$$\alpha = 1 - \left(1 - \frac{2t}{d}\right)^2 \tag{A3}$$

Similarly, we can write the average liquid saturation, using the average flow channel, as

$$\beta = 1 - \left(1 - \frac{2\langle t\rangle}{\langle d_c\rangle}\right)^2 \tag{A4}$$

Here, $\langle t\rangle$ is the average film thickness. Realizing that $\langle d_c\rangle^2/d^2$ is approximately equal to 2 and that $\langle t\rangle\langle d_c\rangle$ is approximately equal to td from continuity considerations, Eq. A4 becomes

$$\beta = 1 - \left(1 - \frac{t}{d}\right)^2 \tag{A5}$$

Eliminating the common factor in Eqs. A3 and A5, we obtain Eq. 13.

LITERATURE CITED

Baker, O., "Simultaneous Flow of Oil and Gas," *Oil Gas J.*, **53**, 185 (1954).

Barnea, D., O. Shoham, and Y. Taitel, "Flow Pattern Transition for Vertical Downward Two Phase Flow," *Chem. Eng. Sci.*, **37**, 741 (1982).

Bird, R. B., W. E. Stewart, and E. N. Lightfoot, *Transport Phenomena*, Wiley, New York (1960).

Beimesch, W. E., and D. P. Kessler, "Liquid-Gas Distribution Measurements in the Pulsing Regime of Two-Phase Concurrent Flow in Packed Beds," *AIChE J.*, **17**, 1,160 (1971).

Charpentier, J. C., and M. Favier, "Some Liquid Holdup Experimental Data in Trickle-Bed Reactors for Foaming and Nonfoaming Hydrocarbons," *AIChE J.*, **21**, 1,213 (1975).

Chou, T. S., F. L. Worley, and D. Luss, "Transition to Pulsed Flow in Mixed-Phase Cocurrent Downflow Through a Fixed Bed," *Ind. Eng. Chem. Proc. Des. Dev.*, **16**, 424 (1977).

Dimenstein, D. M., S. P. Zimmerman, and K. M. Ng, "Trickling and Pulsing Transition in Cocurrent Downflow Trickle-Bed Reactors with Special Reference to Large-Scale Columns," *ACS Symp. Ser.*, 237, 3 (1984).

Froment, G. F., and K. B. Bischoff, *Chemical Reactor Analysis and Design*, Wiley, New York (1979).

Fukushima, S., and K. J. Kusaka, "Interfacial Area and Boundary of Hydrodynamic Flow Region in Packed Column with Cocurrent Downward Flow," *J. Chem. Eng. Japan*, **10**, 461 (1977).

Gianetto, A., et al., "Hydrodynamics and Solid-Liquid Contacting Effectiveness in Trickle-Bed Reactors," *AIChE J.*, **24**, 1,087 (1978).

Hartley, D. E., and W. Murgatroyd, "Criteria for the Break-Up of Thin Liquid Layers Flowing Isothermally Over a Solid Surface," *Int. J. Heat Mass Transfer*, **7**, 1,003 (1964).

Hinze, J. O., "Fundamentals of the Hydrodynamic Mechanisms of Splitting in Dispersion Process," *AIChE J.*, **1**, 289 (1955).

Levich, V. G., *Physicochemical Hydrodynamics*, Prentice-Hall, Englewood Cliffs, NJ (1962).

Lockhart, R. W., and R. C. Martinelli, "Proposed Correlation of Data for Isothermal Two-Phase, Two-Component Flow in Pipes," *Chem. Eng. Prog.*, **45**, 39 (1949).

Norman, W. S., and V. McIntyre, "Heat Transfer to a Film on a Vertical Surface," *Trans. Inst. Chem. Engrs.*, **38**, 301 (1960).

Payatakes, A. C., C. Tien, and R. M. Turian, "A New Model for Granular Porous Media. I: Model Formulation," *AIChE J.*, **19**, 58 (1973).

Sato, Y., et al., "Flow Pattern and Pulsation Properties of Cocurrent Gas-Liquid Downflow in Packed Beds," *J. Chem. Eng. Japan*, **6**, 315 (1973).

Sevik, M., and S. H. Park, "The Splitting of Drops and Bubbles by Turbulent Fluid Flow," *Trans. ASME, J. Fluid Eng.*, **95**, 53 (1973).

Sicardi, S., H. Gerhard, and H. Hoffmann, "Flow Regime Transition in Trickle-Bed Reactors," *Chem. Eng. J.*, **18**, 173 (1979).

Taitel, Y., and A. E. Dukler, "A Model for Predicting Flow Regime Transitions in Horizontal and Near-Horizontal Gas-Liquid Flow," *AIChE J.*, **22**, 47 (1976).

Taitel, Y., D. Bornea, and A. E. Dukler, "Modeling Flow Pattern Transitions for Steady Upward Gas-Liquid Flow in Vertical Tubes," *AIChE J.*, **26**, 345 (1980).

Talmor, E., "Two-Phase Downflow Through Catalyst Beds," *AIChE J.*, **23**, 868 (1977).

Weekman, V. W., Jr., and J. E. Myers, "Fluid-Flow Characteristics of Concurrent Gas-Liquid Flow in Packed Beds," *AIChE J.*, **10**, 951 (1964).

Wijffels, J. B., J. Verloop, and F. J. Zuiderweg, "Wetting of Catalyst Particles under Trickle Flow Conditions," *ACS Monograph Ser.*, 133, 151 (1974).

Manuscript received Apr. 5, 1984, and revision received Apr. 25, 1985.